Ocean Dynamics (2005) 55: 124–136
DOI 10.1007/s10236-005-0004-7

David Pritchard

Suspended sediment transport along an idealised tidal embayment: settling lag, residual transport and the interpretation of tidal signals

Received: 21 January 2005 / Accepted: 20 May 2005 / Published online: 25 August 2005

Abstract We present semi-analytical solutions for suspended sediment concentration (SSC) and residual sediment transport in a simple mathematical model of a short tidal embayment. These solutions allow us to investigate in some detail the characteristic tidal and semi-tidal variation of SSC and the processes leading to residual sediment transport, including settling and scour lags, the roles of 'local' and 'advective' contributions, and the presence of internally or externally generated overtides. By interpreting the transport mechanisms in terms of the classic conceptual models of settling lag we clarify how these models may be expressed in mathematical terms. Our results suggest that settling lag is usually a more important process than scour lag, and that a local model which neglects advection may predict the direction of net sediment transport incorrectly. Finally, we discuss our results in the context of other transport processes and morphodynamic feedback.

Keywords Coastal sediment transport · Tidal asymmetry · Suspension · Settling lag · Scour lag

1 Introduction

The sediment dynamics of tidal embayments have been a matter of practical and scientific interest for many decades. In recent years, new measurement techniques such as acoustic imaging have made it possible to study the short-term processes of sediment transport in some detail, while process-based numerical models have improved in both efficiency and accuracy, to the extent that they can now be used to predict long-term morphodynamical evolution. The processes controlling sediment transport have been revealed to involve the interaction of many complex physical and biological mechanisms. To clarify how these mechanisms operate, though, it is still useful to develop comparatively simple models which describe either in qualitative terms or in very general quantitative terms how the various mechanisms of sediment mobilisation and transport interact to produce residual transport over tidal or longer periods. Such models can guide the interpretation of detailed field or numerical data and contribute to our basic understanding of sedimentary systems.

The first modern conceptual models for suspended sediment transport in tidal systems were developed by van Straaten and Kuenen (1958) and Postma (1961) in their studies of the Wadden Sea. These studies first established the importance of lag effects in suspended sediment transport: the finite time taken for suspended sediment concentration (SSC) to respond to changing current velocity means that spatial or temporal asymmetries in the currents can lead to a net flux of sediment over the course of a tidal cycle. This is generally referred to as *settling lag*, and it may be enhanced when the presence of a threshold shear stress for erosion delays the re-entrainment of sediment into suspension (*scour lag*). A good account of these processes has been given by Nichols and Biggs (1985). Groen (1967) first investigated some aspects of settling lag within a mathematical model, and in recent years a number of studies have sought to elaborate this, considering either the asymmetries caused by the presence of multiple tidal components (e.g. Prandle 1997; Hoitink et al. 2003) or those due to cross-shore bathymetric variations (e.g. Pritchard and Hogg 2003)

When applying conceptual models of lag-driven transport in the field, difficulties arise because SSC signals measured at a point contain contributions from both locally suspended sediment and sediment advected into the study region from elsewhere. It has been recognised for some time that it should be possible to distinguish between these contributions by examining the frequency components of the SSC variation, and

Responsible Editor: Han Winterwerp

D. Pritchard
BP Institute for Multiphase Flow, Department of Earth Sciences, University of Cambridge, Cambridge, CB3 0EZ, UK
E-mail: david@bpi.cam.ac.uk

models of this variation have been developed with varying degrees of mathematical complexity (e.g. Weeks et al. 1993; Bass et al. 2002). A short embayment, such as those originally investigated by van Straaten and Kuenen (1958) and Postma (1961), is a natural laboratory in which to investigate how these components interact, how they may be distinguished, and how tidal asymmetries which are generated bathymetrically combine with those imposed externally to encourage the net accumulation or erosion of sediment.

In this paper, we consider a simple model of such an embayment. By imposing several restrictions on the embayment geometry, we are able to obtain a tractable model in which various transport asymmetries can be investigated mathematically, and related to the purely conceptual models which are of use in field studies of more complicated coastal systems. The dynamical model which we employ is very similar to that used by Schuttelaars and de Swart (1996) to investigate the long-term morphodynamics of embayments: in the current study, however, we employ slightly different sediment transport models, we do not confine ourselves to the case where the excursion of fluid elements is small, and most importantly, we focus our attention on the short-term dynamics of suspended sediment, with the aim of elucidating the transport processes in a way which may readily be related to observational data.

The paper is structured as follows. In Sect. 2, we describe the embayment geometries which we consider; we then derive and discuss a one-dimensional, cross-sectionally integrated sediment transport model. In particular, we discuss the mechanisms affecting the variation of suspended sediment concentrations, and how to obtain solutions to the model. In Sect. 3 we develop and investigate a number of such solutions and calculate the resulting residual sediment transport, and we place our results in the context of existing conceptual models. In Sect. 4, we discuss other transport and morphodynamical feedback mechanisms and their possible interaction with tidal advective transport. Finally, in Sect. 5, we discuss our results and offer some more general conclusions.

2 Construction and properties of the model

2.1 Governing equations

We restrict ourselves to considering embayments with three properties. Firstly, they are short compared to the tidal wavelength, so that the so-called 'pumping flow' solution provides a good approximation to the hydrodynamics. Secondly, they are narrow and shallow compared to their length, so the sediment dynamics may reasonably be described by a one-dimensional, cross-sectionally averaged model, following e.g. Schuttelaars and de Swart (1996) and Friedrichs et al. (1998). Thirdly, and most restrictively, the depth of the embayment is constant along its length. This final

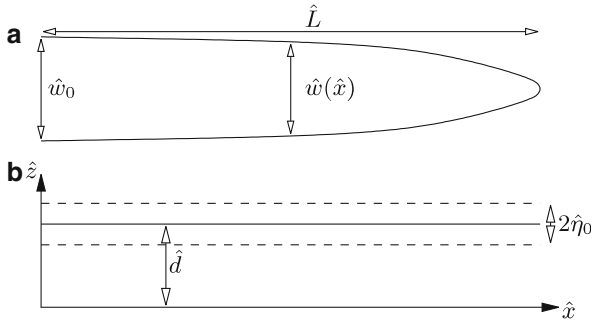

Fig. 1 Schematic of an idealised embayment (lengths not to scale): **a** plan view, **b** longitudinal section. In **b** the *dashed lines* represent high and low tidal elevations; see text for explanation of other legend

restriction is introduced largely for mathematical convenience; in Sect. 4 we will discuss the effect which a more complicated morphology might have.

The geometry of the model is shown in Fig. 1. We take locally Cartesian co-ordinates in which $\hat{x}$ increases inland along the embayment, $\hat{z}$ is vertical and $\hat{y}$ is the transverse horizontal co-ordinate, and we describe the bathymetry of the embayment in terms of its depth $\hat{d}$ below mean sea level and its width $\hat{w}(\hat{x})$. (Throughout, we denote dimensional variables by a caret, while non-dimensional variables are unadorned.) The hydrodynamic variables are the $\hat{x}$-velocity $\hat{u}$, which is taken to be much greater than the transverse or vertical velocities, and the local depth $\hat{h} = \hat{d} + \hat{\eta}$, where $\hat{\eta}$ is the local sea level relative to mean sea level. The embayment is taken to have length $\hat{L}$.

We consider the hydrodynamical regime in which the global Froude number is much less than 1, $F \equiv \hat{U}_0/(\hat{g}\hat{d})^{1/2} \ll 1$ where $\hat{U}_0$ is a characteristic scale for the velocity of the fluid motion. This is equivalent to requiring that the length of the embayment is much smaller than the tidal wavelength. In this regime, sea level is constant to leading order along the embayment at any point in time, and we may employ the conservation of fluid mass to write the 'pumping' approximation to the velocity field (Schuttelaars and de Swart 1996),

$$\bar{u} = (\hat{x}, \hat{t}) = \frac{\mathrm{d}\hat{\eta}}{\mathrm{d}\hat{t}} \frac{\hat{A}(\hat{x})}{\hat{w}(x)(\hat{\eta}(\hat{t}) + \hat{d})} \tag{1}$$

where

$$\hat{A}(\hat{x}) = \int_{\hat{x}}^{\hat{L}} \hat{w}(\hat{x}')\mathrm{d}\hat{x}' \tag{2}$$

and where $\bar{u}$ is the cross-sectionally averaged velocity. (In Sect. 2.3.1, we will discuss the relationship between the hydrodynamics described here and those assumed by van Straaten and Kuenen 1958.)

We also average the mass concentration of suspended sediment $\hat{c}$ over the entire cross-section to obtain $\bar{c}$; the sediment transport equation is then given by

$$\frac{\partial}{\partial \hat{t}}\left[\hat{w}(\hat{\eta}+\hat{d})\bar{c}\right]+\frac{\partial}{\partial \hat{x}}\left[\beta\hat{w}(\hat{\eta}+\hat{d})\bar{u}\bar{c}\right]=[\hat{m}_e q_e-\gamma\hat{w}_s\bar{c}]\hat{w}. \tag{3}$$

Here $\hat{m}_e q_e(\bar{u})$ is a sediment erosion rate averaged over the width of the channel: the dimensional factor $\hat{m}_e$ is chosen such that q_e is of order unity for typical values of $\bar{u}$. We have neglected additional transport mechanisms such as the along-channel dispersion of sediment; in Sect. 4, we will discuss the possible importance of these neglected processes.

Equation 3 contains two 'shape factors'. The first, γ, is a near-bed concentration factor defined by $\gamma = \hat{c}_0/\bar{c}$,where $\hat{c}_0$ is the suspended sediment concentration just above the bed. The second 'shape factor', β, is defined by

$$\beta(\hat{x},\hat{t}) = \frac{1}{\hat{h}(\hat{x},\hat{t})\hat{w}(\hat{x})\bar{u}(\hat{x},\hat{t})\bar{c}(\hat{x},\hat{t})} \times \iint \hat{u}(\hat{x},\hat{y},\hat{z},\hat{t})\hat{c}(\hat{x},\hat{y},\hat{z},\hat{t})\mathrm{d}\hat{y}\mathrm{d}\hat{z}, \tag{4}$$

where the integral is taken over the cross-section $\hat{x} =$ constant.

To evaluate the time- and space-variation of γ and β correctly would require a detailed model of the vertical mixing and redistribution of suspended sediment—for example, using the eddy diffusivity approach recently applied by Jung et al. (2004), or the more physically complex and realistic models of Ross and Mehta (1989) or Winterwerp (2001). This lies beyond the current study; however, by analogy with other vertically-averaged sediment transport models (e.g. Bolla Pitaluga and Seminara 2003) we may obtain a first approximation by setting each shape factor to a constant value, to be calculated using some model of vertical and lateral sediment mixing and settling under steady flow conditions. For sufficiently fine sediment, the suspension will become essentially well-mixed in the water column so that $\beta = 1$ and $\gamma = 1$. As the sediment becomes coarser, concentrations become higher in the low-velocity region close to the bed and so γ increases while β is likely to decrease. Few, if any, direct measurements have been made of the cross-sectional distribution of suspended sediment in tidal embayments, although some recent observations (van de Kreeke and Hibma 2005) suggest that there may be substantial variation across the channel. In the context of estuaries, measurements (e.g. Shi et al. 1997; Shi 2004) and detailed numerical models (e.g. Cancino and Neves 1999) both suggest that this variation is a highly complex process. To make analytical progress without restricting ourselves to a particular model of sediment mixing, we will not introduce a particular model here, but will instead demonstrate how γ may be absorbed by rescaling the governing equations, while we will treat β as an additional parameter of the system and investigate how the results alter as it is varied. However, the coupling between β and E as sediment size is varied should be taken into account when interpreting our results.

Assuming tidal flow with period $2\pi\hat{T}$ and M_2 amplitude $\hat{\eta}_0$, and taking the width scale to be set by the width at the mouth of the embayment $\hat{w}(0) = \hat{w}_0$,we may non-dimensionalise these equations by defining

$$t=\frac{\hat{t}}{\hat{T}},\quad x=\frac{\hat{x}}{\hat{L}},\quad \eta_0=\frac{\hat{\eta}_0}{\hat{d}},\quad \eta=\frac{\hat{\eta}}{\hat{d}},\quad w=\frac{\hat{w}}{\hat{w}_0},\quad u=\frac{\hat{T}\bar{u}}{\hat{L}}\quad\text{and}\quad c=\frac{\gamma\hat{w}_s\bar{c}}{\hat{m}_e}. \tag{5}$$

We obtain

$$u(x,t)=\frac{\mathrm{d}\eta}{\mathrm{d}t}\frac{A(x)}{w(x)(1+\eta(t))},\quad A(x)=\int_x^1 w(x')\mathrm{d}x' \tag{6}$$

and, with judicious simplification,

$$\frac{\partial c}{\partial t}+\beta u\frac{\partial c}{\partial x}=E\frac{q_e-c}{h}+(1-\beta)c\frac{\partial}{\partial x}[uwh], \tag{7}$$

where for convenience we write the total fluid depth $h = 1+\eta$. The parameter E represents the ratio of the tidal timescale to the timescale over which sediment concentrations respond to changes in erosion and deposition rates, and is given by $E = \gamma\hat{w}_s\hat{T}/\hat{d}$.

Table 1 Approximate geometry and corresponding parameter values for two sub-systems of the Wadden Sea inlets studied by Postma (1961), and for the channel system on the Norfolk coast studied by Pethick (1980)

System	Length (est.)	Width (est.)	Min. $\hat{h}$	Max. $\hat{h}$	$\hat{d}$	$\hat{\eta}_0/\hat{d}$	F	$E_{16\ \mu m}$	$E_{32\ \mu m}$	$E_{64\ \mu m}$	$E_{128\ \mu m}$
Friese Wad/Danzig Gat	12 km	0	0	1.6 m	0.8 m	1.0	0.62	1.98	7.91	31.0	126.4
(stations 5–8)		100 m	1.8 m	4.5 m	3.15 m	0.43	0.31	0.50	2.01	7.86	32.1
		300 m	4.7 m	7.3 m	6.0 m	0.22	0.23	0.26	1.05	4.13	16.9
		1000 m	7.9 m	9.8 m	0.95 m	0.11	0.19	0.18	0.72	2.80	11.4
Amsteldiep	9 km	1 km	0.15 m	1.9 m	1.0 m	0.85	0.41	1.54	6.17	24.2	98.7
(stations 11–13)		1 km	5.4 m	6.8 m	6.1 m	0.11	0.17	0.26	1.04	4.06	16.6
		1 km	6.3 m	7.8 m	7.05 m	0.11	0.16	0.22	0.90	3.51	14.3
Warham (mouth	800 m	5 m	0.4 m	1.6 m	1.0 m	0.6	0.04	1.58	6.33	24.8	101.1
to headwater)		10 m	0.5 m	2.0 m	1.25 m	0.6	0.03	1.27	5.06	19.8	80.9

Depths are taken from Postma's Table 1 and Pethick's Table 4; widths and lengths estimated from Postma's Figs. 2 and 3 and Pethick's Fig. 2. The values of E are calculated taking $\gamma = 1$ (and so are effectively minimum estimates), for the effective sediment sizes 16, 32, 64 and 128 μm. The data are not sufficient to estimate β. Note that stations 5 (Friese Wad) and 11 (Amsteldiep) are each on the tidal flats at the end of the channel rather than in the channel itself

Table 1 shows some illustrative examples of small tidal embayments, taken from the study by Postma (1961) of Wadden Sea inlets, and from the study by Pethick (1980) of tidal propagation in the rather smaller Warham channel system in the Stiffkey marshes on the coast of Norfolk. It is clear from the data presented here that the idealisation of an inlet of constant depth is a strong simplification of the geometry of the Wadden Sea inlets; it is also a simplification of the Warham channel. However, the data provided by Postma do allow us to identify relevant parameter regimes.

Calculating the Froude number F using local values of $\hat{d}$ indicates that the 'pumping' approximation (Eq. 6) is likely to be reasonable except in the inner reaches of the Wadden Sea inlets, where the depth becomes very small and the corresponding tidal wavelength is reduced. In these regions we may also expect frictional effects to be important, but overall, we may follow Schuttelaars and de Swart (1996) in concluding that the short embayment condition is marginally satisfied in these systems. In the Warham channel, the condition is more strongly satisfied. Meanwhile, in each system the tidal amplitude may be a significant fraction of the mean water depth even within the channel, allowing strong tidal asymmetries to develop: this will be discussed in Sect. 2.2.

The parameter E, which controls lag effects, varies strongly with the sediment properties and embayment geometry: recalling that $\gamma \geq 1$, we may find values of E as low as $E \approx 0.1$ or as high as $E \gtrsim 100$, even for relatively fine sediment.

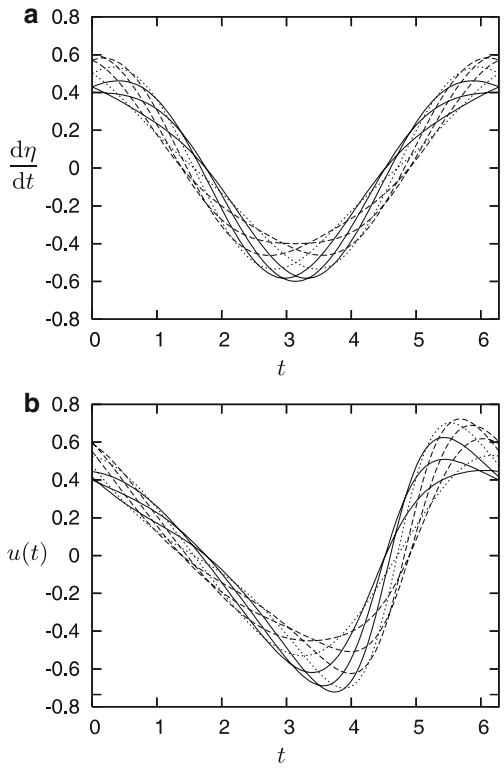

Fig. 2 **a** Externally imposed and **b** actual tidal signals for $\eta(t) = (1/2)[\sin t + 0.1\sin(2t + \phi)]$, where $\phi = \pi/2$ or $3\pi/2$ (*dotted lines*), $\pi/2 < \phi < 3\pi/2$ (*solid lines*) and $3\pi/2 < \phi < 5\pi/2$ (*dashed lines*)

2.2 Internal and external tidal asymmetry

An important point about the pumping flow solution (Eq. 6) is that it represents the generation of overtides in the fluid velocity by the interaction between the external tidal forcing and the bathymetry. This is easily demonstrated: at any point in the embayment the velocity $u(x,t)$ is proportional to $\dot{\eta}/(1+\eta)$, and this means that even with sinusoidal external forcing $\eta(t) = \eta_0 \sin t$, the currents develop a slack water asymmetry, with higher accelerations (shorter slack water) around low tide than around high tide. This may be expected (Groen 1967) to lead to higher concentrations on the flood than on the ebb and thus to enhance landwards transport; however, it is not clear in advance how much this effect is offset by faster settling in the shallower water at low tide. This is one question which will be answered below.

When a small overtide is present in the external forcing, so $\eta(t) = \eta_0[\sin t + \epsilon \sin(2t + \phi)]$ for some phase angle ϕ and small relative amplitude ϵ, the resulting current time series can become rather complicated (Figs. 2, 3).

The external tide is ebb-dominated (higher peak ebb than peak flood velocities) for $\pi/2 < \phi < 3\pi/2$, and flood-dominated for $0 < \phi < \pi/2$ and $3\pi/2 < \phi < 2\pi$ (Fig. 3a). The actual tidal flow experienced in the embayment is similarly ebb-dominated for $\pi/2 < \phi < 3\pi/2$ and flood-dominated for $0 < \phi < \pi/2$ and $3\pi/2 < \phi < 2\pi$ (Figs. 2b, 3b). However, whereas the external tide has a longer high water slack (HWS) for $0 < \phi < \pi$ and a longer low water slack (LWS) for $\pi < \phi < 2\pi$, the embayment geometry tends to decrease the length of LWS. Consequently, LWS is shorter than HWS for all values of ϕ, though this trend is strongest for $0 < \phi < \pi$. Additionally, the peak velocities on both flood and ebb are higher when LWS is short than when it is long, thus increasing still further the tendency for higher concentrations on the flood, and so enhancing the trend towards landwards transport with decreasing length of LWS.

2.3 Characteristic form of the sediment transport equation

In characteristic form, the sediment transport equation becomes

$$\frac{dc}{dt} = E\frac{q_e - c}{h}\bigg|_{x=x_c} + (1-\beta)c\frac{\partial}{\partial x}[uwh]\bigg|_{x=x_c}$$
$$\text{on characteristics } \frac{dx_c}{dt} = \beta u(x_c, t). \tag{8}$$

It is straightforward to integrate the equation for $x_c(t)$:

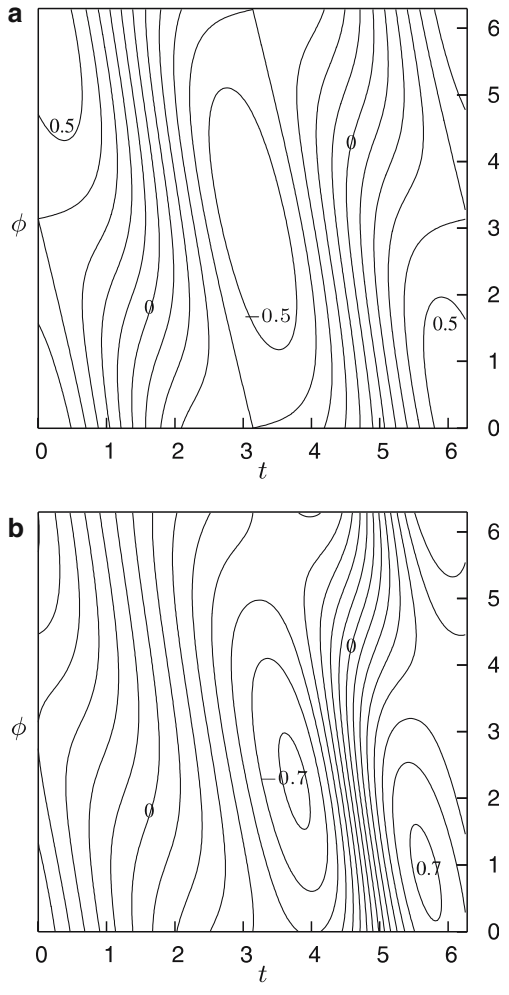

Fig. 3 **a** Externally imposed tidal signal $\mathrm{d}\eta/\mathrm{d}t$ and **b** actual tidal signal $u = \dot{\eta}/(1+\eta)$ for $\eta(t) = (1/2)[\sin t + 0.1\sin(2t+\phi)]$. In (**a**) the contours are at −0.5 to 0.5 by 0.1; in (**b**) they are from −0.7 to 0.7 by 0.1

$$\frac{\mathrm{d}x_c}{\mathrm{d}t} = \beta \frac{\partial \eta}{\partial t} \frac{1}{1+\eta(t)} \frac{A(x_c)}{w(x_c)} \tag{9}$$

and so

$$\int^{x_c} \frac{w(x')\mathrm{d}x'}{A(x')} = \beta \int^{t} \frac{\dot{\eta}(t')\mathrm{d}t'}{1+\eta(t')}; \tag{10}$$

then, since we have $w(x) = -\mathrm{d}A/\mathrm{d}x$, we can integrate both sides to obtain

$$A(x_c) = \frac{K}{(1+\eta(t))^{\beta}} \tag{11}$$

where K is some constant of integration. Whether further analytical progress can be made depends on whether (11) can be inverted explicitly to yield $x_c(t)$: in the remainder of this paper we will confine the discussion to some particular cases (algebraically widening embayments) in which it can.

Equation 8 can be interpreted in terms of the physical mechanisms controlling local suspended sediment concentrations. We note that when $\beta = 1$ the characteristic curves $x_c(t)$ become the trajectories of Lagrangian fluid elements and the final term on the right hand side disappears, so the equation describes the erosion and deposition of sediment by a moving fluid element (c.f. Pritchard and Hogg 2003).

When $\beta \neq 1$ (we will assume for the moment that $\beta < 1$), two differences are made. One is that the characteristic speed $\mathrm{d}x_c/\mathrm{d}t$ is reduced by a factor β: in other words, a 'signal' of SSC no longer propagates at the same speed as the fluid, and instead, sediment is advected on average more slowly than fluid mass. The other effect of this differential advection of sediment and water is to introduce a third 'source' term on the right hand side. The effect of this term depends on the sign of $\partial(uwh)/\partial x$, in other words on whether the flow is locally diverging or converging in the horizontal. When flow is converging at a particular location, water is arriving there more rapidly than sediment, and so suspended sediment concentrations tend to become diluted; conversely, at points of flow divergence, there is a tendency for sediment to be left behind and so for SSC to increase. (These trends are reversed if $\beta > 1$.)

In the context of a short embayment, the horizontal convergence of water corresponds to periods of rising sea level, in other words to the flood tide, so for $\beta < 1$ this differential advection effect will tend to reduce landwards residual transport somewhat: we will observe this effect later (Sect. 3.1.2). It is also interesting to note that a tendency for sediment to be concentrated or diluted by local flow convergence and divergence was observed in the estuarine model of Friedrichs et al. (1998), which employed a cross-sectionally averaged description of sediment transport, but made slightly different assumptions about the relationship between integrated SSCs and deposition rates.

2.4 Explicit solutions for $x_c(t)$ in an algebraically widening embayment

When the embayment widens algebraically towards the mouth, so $w(x) = (1-x)^m$ for some $m \geq 0$, Eq. 11 becomes

$$A(x_c) = \frac{(1-x)^{m+1}}{m+1} = \frac{K}{(1+\eta(t))^{\beta}} \tag{12}$$

and so we may obtain

$$x_c(t;x_0) = 1 - \frac{1-x_0}{(1+\eta(t))^{\beta/(m+1)}} \tag{13}$$

and

$$u(x_c,t) = \frac{(1-x_0)}{m+1} \frac{\dot{\eta}(t)}{(1+\eta(t))^{1+\beta/(m+1)}}, \tag{14}$$

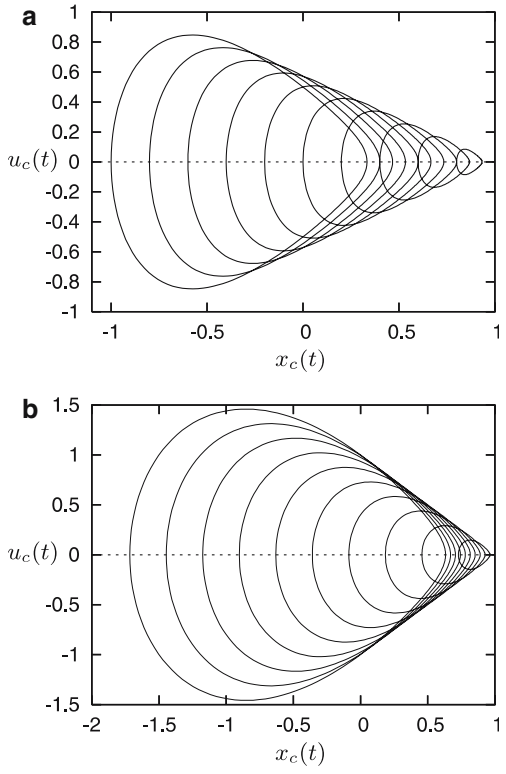

Fig. 4 Selected characteristic curves in the (x,u) phase plane for pumping flow in a rectangular embayment with $\eta(t)=0.5\sin t$ and $\beta=1$: (**a**) actual characteristic curves $x_c(t)$; (**b**) characteristics as modelled by van Straaten and Kuenen (1958)

where x_0 is the position of the characteristic when $\eta=0$, i.e. at mean sea level.

Figure 4a illustrates these characteristics in the (x, u) phase plane. Both the tidal excursion and the maximum velocity decrease landwards, which we may expect to encourage landwards residual sediment transport (Pritchard and Hogg 2003).

From Eq. 13 we can also determine the region of the embayment which is directly affected by a boundary condition on SSC imposed at the mouth. This region is bounded inland by the landmost position of the characteristic which at its seamost position is at $x=0$; it is given by

$$0 \le x \le 1 - \left(\frac{1-\eta_-}{1+\eta_+}\right)^{\beta/(m+1)}, \tag{15}$$

where $\min_t \eta(t) = -\eta_-$ and $\max_t \eta(t) = \eta_+$. Note that as β decreases (less well-mixed suspensions) or m increases (a more rapidly widening embayment), a smaller portion of the embayment is directly affected by the seaward boundary. In a state of morphodynamic equilibrium the dynamics of the inner and outer embayment must of course be strongly coupled; however, this observation may be important when considering the response of a system to abrupt changes in forcing. In what follows we will neglect the effect of any seaward boundary condition, but the possibility of such effects should be remembered.

It is also interesting to compare the characteristics defined by Eqs. 13 and 14 with the fluid trajectories derived by van Straaten and Kuenen (1958). They required that the tidal curve should be sinusoidal and that the amplitude of velocity variation should increase linearly with distance from the head of the embayment. In our notation this becomes $u(x,t)=(1-x)\cos t$, and so the Lagrangian fluid trajectories are

$$x_{\mathrm{L}}(t;x_0) = 1 + (x_0 - 1)\mathrm{e}^{-\sin t}. \tag{16}$$

Several of these trajectories are plotted in Fig. 4b, and it can be seen that they are roughly similar to the characteristics $x_c(t)$ obtained by assuming 'pumping' flow; in particular, the graphical argument employed by van Straaten and Kuenen to deduce residual landwards transport is essentially unaffected by the change. (As a point of interest, in a rectangular embayment it is possible for pumping flow to give the velocity field assumed by van Straaten and Kuenen (1958), but only if the imposed tidal elevation curve is non-sinusoidal: if we require that $1+\eta(t) = k\mathrm{e}^{\sin t}$ for some constant k, then the pumping flow approximation (Eq. 6) yields Eq. 16.)

2.5 Separable solutions when $q_e \propto |u|^n$

When $q_e \propto |u|^n$ and $w(x)=(1-x)^m$ for some exponents $n > 0$ and $m \ge 0$, the concentration field may be written in a very convenient form. In this case, we have

$$u(x,t) = \frac{\dot\eta}{1+\eta}\frac{A}{w} = \frac{\dot\eta}{1+\eta}\frac{(1-x)}{m+1} \tag{17}$$

and substituting this into Eq. 7, we obtain

$$\frac{\partial}{\partial t}[(1+\eta)(1-x)^m c] + \frac{\partial}{\partial x}\left[\beta\frac{(1-x)^{m+1}}{m+1}c\frac{\mathrm{d}\eta}{\mathrm{d}t}\right] = E\left|\frac{\dot\eta}{1+\eta}\right|^n\left(\frac{1-x}{m+1}\right)^n(1-x)^m - Ec(1-x)^m. \tag{18}$$

We now seek solutions of the form $c(x,t)=\Xi(x)\Phi(t)$: substituting this in, we obtain

$$\Xi(x)(1-x)^m\Phi(t)\frac{\mathrm{d}\eta}{\mathrm{d}t} + \Xi(x)(1-x)^m(1+\eta)\frac{\mathrm{d}\Phi}{\mathrm{d}t} + \beta\Phi(t)\frac{\mathrm{d}\eta}{\mathrm{d}t}\frac{\mathrm{d}}{x}\left[\frac{(1-x)^{m+1}}{m+1}\Xi(x)\right] = E\left|\frac{\dot\eta}{1+\eta}\right|^n\left(\frac{1-x}{m+1}\right)^n(1-x)^m - E\Xi(x)\Phi(t)(1-x)^m. \tag{19}$$

This equation is separable if

$$(1-x)^m \Xi(x) \propto \frac{\mathrm{d}}{\mathrm{d}x}\left[(1-x)^{m+1}\Xi(x)\right] \propto (1-x)^{m+n}, \quad (20)$$

and this can be satisfied if we take $\Xi(x)=(1-x)^n$. We then obtain an ordinary differential equation for $\Phi(t)$,

$$(1+\eta)\frac{\mathrm{d}\Phi}{\mathrm{d}t} + \left[\frac{\mathrm{d}\eta}{\mathrm{d}t} - \beta\frac{\mathrm{d}\eta}{\mathrm{d}t}\left[\frac{m+n+1}{m+1}\right] + E\right]\Phi(t) = \frac{E}{(m+1)^n}\left|\frac{\dot{\eta}}{1+\eta}\right|^n. \quad (21)$$

It is simple (see Pritchard and Hogg (2003) Sect. A) to obtain periodic solutions to Eq. 21 which can be expressed as integrals and readily evaluated numerically. We can then calculate the net flux per unit width through a cross-section,

$$Q(x) \equiv \frac{1}{w(x)}\int_0^{2\pi} \beta c(x,t)h(t)w(x)u(x,t)\mathrm{d}t \quad (22)$$

$$Q(x) = \frac{\Xi(x)A(x)}{w(x)}\int_0^{2\pi} \beta\Phi(t)\frac{\mathrm{d}\eta}{\mathrm{d}t}\mathrm{d}t \quad (23)$$

$$Q(x) = Q_0\frac{(1-x)^{n+1}}{m+1} \quad \text{where} \quad Q_0 \equiv \int_0^{2\pi} \beta\Phi(t)\frac{\mathrm{d}\eta}{\mathrm{d}t}\mathrm{d}t. \quad (24)$$

An important advantage which these solutions posses is that the residual sediment transport can now be characterised by the single quantity Q_0 rather than by a function $Q(x)$; this makes it relatively easy to investigate their dependence on the governing parameters of the model.

3 Some particular solutions and their interpretation

We are now in a position to develop solutions for the variation of SSC, either by seeking solutions to Eq. 21 or—for more general forms of the erosion rate—by integrating the characteristic equations (Eqs. 8). Having developed such solutions, we may then calculate the residual flux of sediment $Q(x)$ over a tide, and interpret the trends in terms of the various asymmetries and processes identified in the preceding section. In fact, the patterns of residual transport do not appear to be greatly sensitive to the precise form of the erosion rate $q_e(u)$, and so we will generally confine ourselves to investigating solutions of separable type, for which the residual transport can be described by the single quantity Q_0. The exception occurs when we examine the effect of scour lag, when we must employ the more general formulation to allow for an erosion threshold.

We will first consider transport under a sinusoidal external tide (Sect. 3.1), considering in turn the significance of various components of the model; we will then briefly investigate how the presence of externally imposed overtides modifies the residual transport (Sect. 3.2).

3.1 Transport under a sinusoidal external tide

The simplest case which we can consider occurs when the externally imposed tidal elevation is sinusoidal, $\eta(t) = \sin t$. In this case, the asymmetries which drive residual sediment transport are the bathymetrically generated overtides discussed in Sect. 2.2, the difference in depths at HWS and LWS, and the spatial gradient of velocity.

3.1.1 Temporal variation of SSC: local and advective processes

Several mathematical models which have investigated the effect of tidal asymmetry on net sediment transport (e.g. Groen 1967; Prandle 1997; Hoitink et al. 2003) have implicitly or explicitly neglected the changes to SSC which occur as higher and lower 'background' concentrations are advected past the measurement point. This advective contribution to the variation of SSC is known to be important in several shelf sea environments, and may be identified in time series by a simple rule of thumb: the advection back and forth of a background gradient of SSC should give a variation at tidal frequency, while contributions from local erosion and deposition depend on the magnitude but not the direction of currents, and so will vary at twice this frequency (Weeks et al. 1993). Even the assumption of a basic background gradient of SSC (e.g. Bass et al. 2002) may be something of a simplification in a dynamic coastal environment, and so it is interesting to compare the predictions of our model including advection with those of a model which neglects advection and assumes only local contributions to SSC.

We can obtain a local model by setting $\beta=0$ in Eq. 21, obtaining

$$(1+\eta)\frac{\mathrm{d}\Phi}{\mathrm{d}t} + \left[\frac{\mathrm{d}\eta}{\mathrm{d}t} + E\right]\Phi = \frac{E}{(m+1)^n}\left|\frac{\dot{\eta}}{1+\eta}\right|^n. \quad (25)$$

Figure 5 compares some typical solutions of this equation with those when advection is included: the character of the results and the importance of advection both depend on the value of the exchange rate parameter E.

When $E \ll 1$ (Fig. 5a), corresponding to fine sediment and thus a slow sediment response time, the main variation is due to the advection of a background SSC gradient which itself arises as a long-time average of local erosion and deposition. This background concentration increases seawards with the higher velocities, and so concentrations are highest around HWS and lowest around LWS. The basic variation of SSC predicted by a

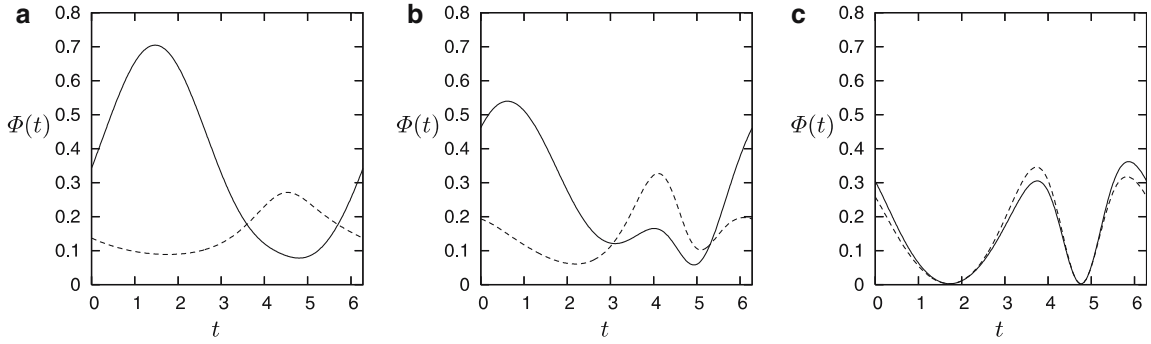

Fig. 5 Time series $\Phi(t)$ for suspended sediment concentration with $m=0$, $n=2$, $\beta=1$ and (**a**) $E=0.1$; (**b**) $E=1$; (**c**) $E=10$. *Solid lines* show solutions including advective contribution; *dashed lines* show solutions neglecting it. The external tidal forcing is $\eta(t)=(1/2)\sin t$

non-advective model is also at the tidal frequency, because the sediment responds too slowly to be affected by higher-frequency velocity components, but it is almost precisely out of phase with the advective signal because peak velocities occur either side of the short LWS, maintaining high concentrations throughout the slack.

As E increases, local contributions become increasingly important, though as Fig. 5b indicates, for $E = O(1)$the advective component is still dominant. It is only for relatively coarse sediment, $E \gg 1$ (Fig. 5c), that the semi-tidal signal of local erosion and deposition becomes dominant. Even in this regime, however, advection modifies the relative sizes of the flood and ebb peaks in SSC, and this exerts a significant control on the residual flux over a cycle. (This demonstrates the difficulty of assessing the importance of sediment transport mechanisms solely from correlations between velocity and concentration data.)

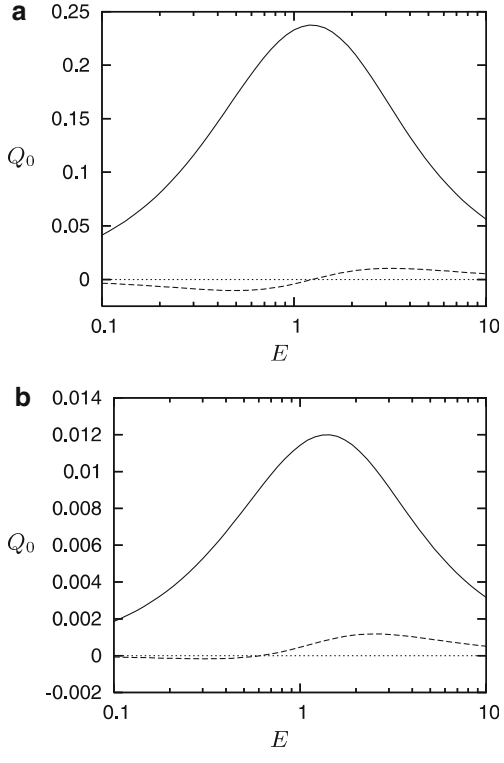

Fig. 6 Residual flux Q_0 of suspended sediment through an embayment with $\beta=1$ and **a** $m=0$, $n=2$; **b** $m=1$, $n=3$. *Solid lines* show solutions including advective contribution; *dashed lines* show solutions neglecting it. The external tidal forcing is $\eta(t)=(1/2)\sin t$

Figure 6 compares the residual fluxes Q_0 predicted by the advective and non-advective models for various parameter values. Even in the regime $E \gg 1$, there is an order of magnitude difference between the fluxes predicted accounting for and neglecting advection, and for $E \lessapprox 1$ even the direction of net transport may be incorrectly predicted by the non-advective model. This emphasises the importance of cross-shore variations in sediment dynamics for conceptual models of transport in these systems—spatial, as well as temporal, lag effects are crucial, as the advection of higher concentrations inland on the flood, followed by their deposition at HWS, promotes a systematic landward movement of sediment (c.f. van Straaten and Kuenen 1958; Pritchard and Hogg 2003).

3.1.2 Sensitivity of results to sediment transport model and embayment geometry

In our simple embayment model, there are two parameters which describe the geometry: the exponent m which determines the rate at which it widens, and the relative amplitude η_0 of the tidal amplitude. Additionally, the sediment transport model is characterised by the exponent n in the erosion rate and by the shape factor β in the sediment flux term.

A brief parameter study (omitted here for brevity) suggests that although the values of the parameters m and n have an important effect on the magnitude of the residual fluxes, they do not greatly affect the trends in sediment transport (c.f. Fig. 6a, b). The variations with η_0 and with β are of more interest.

Figure 7a shows how the residual flux varies with the relative amplitude η_0 of the tide. The most noticeable trend is the strong increase of residual transport as η_0 increases and the internally-generated tidal asymmetries which drive net transport are strengthened. Additionally, the peak of Q_0 occurs at lower values of E as η_0 is

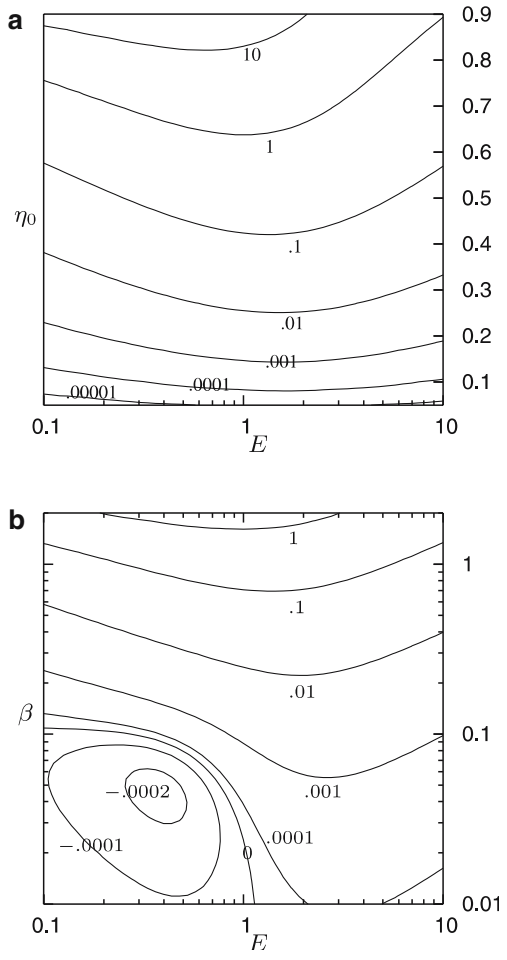

Fig. 7 Residual flux Q_0 as a function of: **a** E and η_0, for $\beta = 1$, $m = 0$ and $n = 2$; **b** E and β, for $\eta_0 = 0.5$, $m = 0$ and $n = 2$ (see contour labels for the values of Q_0)

increased, with this trend being most prominent for larger η_0. This can be explained physically: for large values of η_0, the water is sufficiently shallow at LWS that unless the sediment is very fine, a large amount of it will settle out; this tends to reduce overall concentrations, and thus residual fluxes, for coarser material and so the residual transport becomes more biased towards fine sediment. The overall suggestion from Fig. 7a is that in an embayment under sinusoidal tidal forcing, significant residual transport by tidal advection occurs only if the tidal range is a substantial proportion of the embayment depth. (This is the regime in which the asymptotic model of Schuttelaars and de Swart (1996), based on the assumption of small tidal excursion, is least accurate.)

The role of the advection parameter β is more subtle. Figure 7b illustrates that while the value of β does not greatly affect the value of E for which Q_0 is maximised, it exerts a strong control on the magnitude of the residual flux: this control is stronger than the linear dependence introduced by the factor of β in the definition of Q_0, and indeed, as we have already seen (Fig. 6a), for sufficiently low β and E the direction of residual transport can be reversed. (We recall that the sediment size increases, we expect β to decrease and E to increase; consequently, the parameter regime in which $Q_0 < 0$ may not be experienced in most systems by any class of sediment. It will, however, be accessed by models which neglect advective transport.)

The variation of Q_0 with β may be interpreted in terms of the differential advection mechanism described in Sect. 2.3. During the flood, there is a horizontal convergence of fluid, so for $\beta < 1$ there is a dilution of sediment concentrations and overall a lower landward flux; conversely, during the ebb there is a horizontal divergence of fluid, and differential advection of sediment leads to higher concentrations and overall a higher seaward flux. Consequently, the net effect of a shape factor $\beta < 1$ is to promote the export of sediment through the differential advection mechanism, while a shape factor $\beta > 1$ enhances the ability of the embayment to trap sediment. The contribution of differential advection is strongest for moderately fine sediment (E between about 0.1 and 1). This is because for coarser sediment, it is swamped by the rapid variations in SSC due to erosion and deposition during the tidal cycle, while for finer sediment, the amount of settling is too small to produce significant residual transport.

3.1.3 *The effect of scour lag*

To investigate the effect of scour lag it is necessary to consider an erosion formulation which incorporates a threshold for sediment entrainment. The simplest formulation which has this property is Partheniades' (1965) model for the erosion of cohesive material, which with suitable non-dimensionalisation may be written as

$$q_e(u) = \begin{cases} u^2 - u_e^2 & \text{when } \mid \mathrm{u} \mid > \mathrm{ue}, \\ 0 & \text{otherwise.} \end{cases} \tag{26}$$

For simplicity we will confine ourselves to rectangular embayments, $m = 0$, although it is simple to generalise the results presented here. To develop the solutions for SSC, we write the sediment transport equation in characteristic form. We have already calculated the characteristic trajectories $x_c(t)$, which are given by Eq. 13; the equation for $c(t)$ along a characteristic then becomes

$$\frac{\mathrm{d}c}{\mathrm{d}t} = a(t) - b(t)c(t),$$

where

$$b(t) = \frac{E + (1-\beta)\eta_0 \cos t}{1 + \eta_0 \sin t} \tag{27}$$

and

$$a(t) = \frac{E}{1 + \eta_0 \sin t} q_e\left(\frac{(1-x_0)\eta_0 \cos t}{(1 + \eta_0 \sin t)^{1+\beta}}\right). \tag{28}$$

Following Pritchard and Hogg (2003) (Sect. A), we may obtain periodic solutions to this equation and calculate the corresponding residual fluxes $Q(x)$.

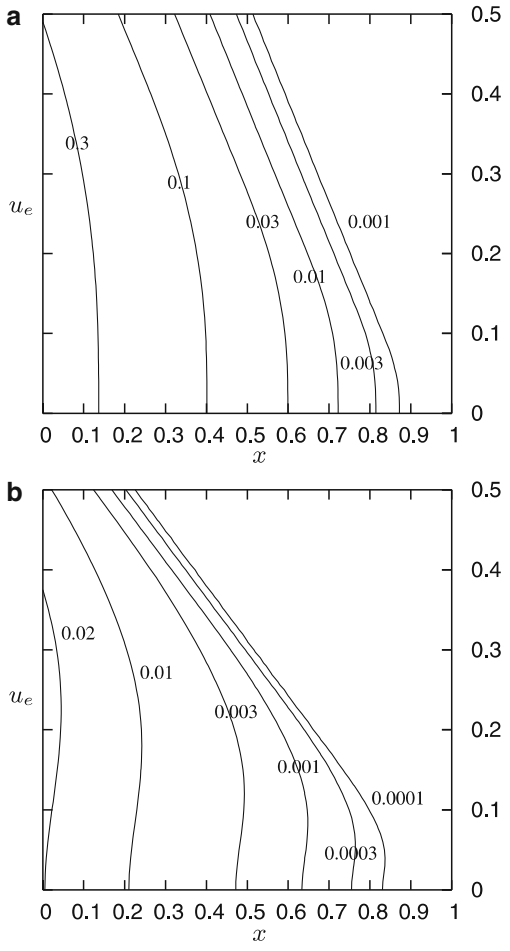

Fig. 8 Residual flux $Q(x)$ as a function of position x and of the threshold velocity for erosion u_e, for a rectangular embayment with $\eta(t) = (1/2)\sin t$ and sediment with $E = 1$, $q_e = u^2 - u_e^2$ and (**a**) $\beta = 1$; (**b**) $\beta = 0.25$. No sediment is mobilised landwards of a line $x = x_e(u_e) = 1 - u_e/\sqrt{3}$ in this case. See contour labels for the values of $Q(x)$

Some representative results are shown in Fig. 8. As for the separable solutions which occur when $u_e = 0$, the SSC at an instant (not plotted here for brevity) increases monotonically with distance seawards, as does the residual flux shown here. When $\beta = 1$ (Fig. 8a), settling lag dominates the dynamics: the only noticeable effect of increasing the erosion threshold u_e is to reduce the erosion rate, and consequently the overall levels of SSC and the magnitude of net fluxes. In particular, sediment mobilisation can only occur seawards of the point $x = x_e(u_e) = 1 - u_e\eta_0/\sqrt{1-\eta_0^2}$.

However, when β is rather lower, so local dynamics become more important, scour lag starts to contribute to the residual transport. This can be seen in Fig. 8b, where close to the mouth of the embayment the fluxes actually increase slightly with increasing u_e—at least until u_e becomes large enough to reduce overall SSC significantly. These results suggest that scour lag is a minor factor in contributing to residual landwards transport, but it should not be ignored in situations where transport is controlled by local processes.

3.2 Transport under externally imposed overtides

As we have already noted, when the externally imposed tidal signal includes even a small overtide, a rather complex signal results within the embayment. In particular, the direction of peak current velocities may become biased towards the export of sediment, and the magnitude of slack water asymmetries depends considerably on the relative phase of the overtide (Fig. 3b). We may expect relatively coarse sediment, for which $E \gg 1$, to be most strongly affected by the direction of peak currents, since in this regime there is practically no lag time and the instantaneous sediment flux becomes effectively an instantaneous, super-linear function of velocity, $q \propto u^{n+1}$; however, the behaviour of finer sediment may be more subtle.

Figures 9a and 10a show how the net flux Q_0 varies with the exchange rate parameter E and with the phase ϕ of the imposed overtide. The most important point is that the transport is landwards in most of the parameter space: for sufficiently fine sediment $Q_0 > 0$ regardless of the value of ϕ, although for sufficiently coarse particles the export of sediment is possible (in contrast to the case of a sinusoidal imposed tide, Fig. 6).

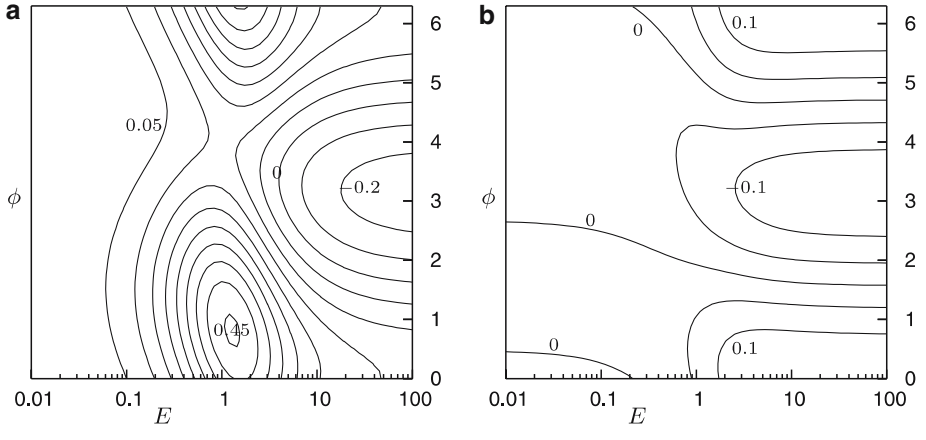

Fig. 9 Residual flux Q_0 through an embayment with $m = 0$, where the external tide has the form $\eta(t) = (1/2)[\sin t + 0.1\sin(2t + \phi)]$, and where we take $n = 2$ and $\beta = 1$: **a** solution with advection; **b** solution neglecting advection. In **a**, contours are at −0.1 to 0.45 by 0.05 and in **b** contours are at −0.1 to 0.1 by 0.05

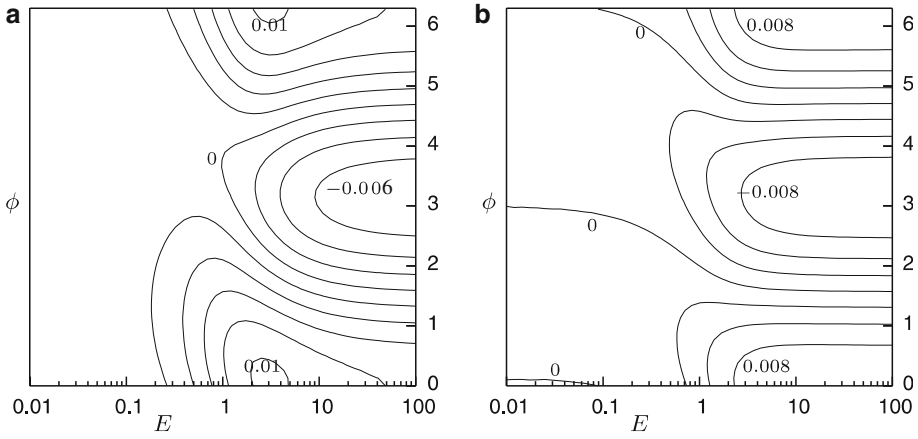

Fig. 10 Residual flux Q_0 through an embayment with $m=0$ and $d=5$, where the external tide has the form $\eta(t)=(1/5)[\sin t+0.1\sin(2t+\phi)]$, and where we take $n=2$ and $\beta=1$: **a** solution with advection; **b** solution neglecting advection. In **a**, contours are at -0.006 to 0.01 by 0.002 and in **b** contours are at -0.006 to 0.006 by 0.002

For $E \gg 1$, as predicted, the transport direction is dominated by the direction of peak velocity (c.f. Fig. 3b). For $E \ll 1$, on the other hand, settling lag effects are considerable, promoting the landward movement of sediment.

The importance of advection may be seen by comparing Figs. 9a and 10a with the corresponding Figs. 9b and 10b, which show the net flux Q_0 as calculated when variations to SSC caused by the advection of sediment are ignored. As in Fig. 6, the neglect of advection is of key importance, especially for finer sediment. One lag effect (the shorter duration of LWS, encouraging higher concentrations on the flood) is still present, and promotes landward transport, but this is swamped by the effect of lower depths (and thus greater settling) at LWS, so that in the non-advective model the transport of fine sediment is biased seawards. When the embayment is deeper, this effect is reduced, but the non-advective model is still seriously misleading (c.f. Fig. 10a, b).

4 Discussion: settling lag and 'balancing' mechanisms

This study has investigated a single mechanism: the tidal advection of sediment and the corresponding residual transport driven by settling lag. In reality, other mechanisms may contribute to the residual transport of sediment; additionally, it may be expected that over time the bathymetry of an embayment will evolve in such a way that residual transport is reduced, and a state of morphodynamic equilibrium or quasi-equilibrium results.

One mechanism which we have neglected is the longitudinal dispersion of sediment. In a cross-sectionally averaged model, this arises not only directly through turbulent mixing in the longitudinal direction, but also indirectly through shear dispersion when sediment is mixed across a cross-section (see e.g. Young and Jones 1991). Such a mechanism was included, for example, in the model of Schuttelaars and de Swart (1996).

Without employing a detailed model of the turbulent mixing and velocity structure across a cross-section, we may still obtain a rough estimate of the relative importance of advective and diffusive transport. The condition for advective transport to dominate is that the advective flux $\bar{u}\bar{c}$ is much greater than the longitudinal dispersive flux $\hat{\kappa}_{\text{eff}}\partial\bar{c}/\partial\hat{x}$, where $\hat{\kappa}_{\text{eff}}$ is an effective diffusion coefficient. A simple estimate of $\hat{\kappa}_{\text{eff}}$ for dissolved tracers has been provided by Smith (1977), who found that $\hat{\kappa}_{\text{eff}} \sim k\hat{w}^2\bar{u}/\hat{d}$, where k is a coefficient of order unity or smaller. (For a parabolic channel, Smith found theoretically that $k=0.096$, and when fitting results to the River Colne the combined effects of channel curvature and salinity gradients reduced dispersion further to $k=0.03$.) Assuming that a similar dispersion law holds for suspended sediment, advective transport will dominate diffusive transport if

$$\frac{1}{\hat{L}}\frac{k\hat{w}^2\hat{L}}{\hat{d}\hat{T}} \ll \frac{\hat{L}}{\hat{T}}, \quad \text{i.e. } \hat{L}\hat{d} \gg k\hat{w}^2. \tag{29}$$

Taking representative values of $k=0.1$, and dimensions for the Wadden Sea embayments of $\hat{L}=10\,\text{km}$ and $\hat{d}=5\,\text{m}$ (c.f. Table 1), we find that we may neglect dispersion if the width of the channel is of the order of 100 m or less; the corresponding values for the Stiffkey marsh channels are $\hat{L}=1\,\text{km}$ and $\hat{d}=1\,\text{m}$, so again dispersion may be neglected for $\hat{w} \ll 100\,\text{m}$—a condition which is easily satisfied. These estimates suggest that at least for cases resembling the narrower systems described in Table 1, the use of an advective model to explain transport phenomena at leading order is justified. However, we note that this scaling does not preclude the possibility that diffusive effects may be locally important (for example, in regions of high local turbulence) or that they may be less reduced than advective fluxes by cancellation, and so contribute systematically under some circumstances to long-term transport.

Another mechanism neglected here, which is difficult to parameterise but which may be especially important over shallow tidal flats, is the mobilisation of sediment by wind-generated waves. Dronkers (1986) proposed that the resuspension of sediment over tidal flats at high water could substantially alter net sediment fluxes, while Ridderinkhof (1998) found in a numerical study

of the Ems–Dollard basin that including wind-waves led to substantially higher concentrations in shallow inshore regions, and thus to a net diffusive flux of sediment out of the basin, balancing lag-driven shorewards transport. The effect of this resuspension on the advective component of transport is harder to predict in advance. If resuspension occurs principally in regions which are only inundated around high water, then it should encourage the offshore advection of sediment as concentrations will be higher on the ebb than on the flood. If the embayment is shallow enough, on the other hand, significant resuspension may have taken place everywhere at low water, enhancing SSC on the flood and promoting landwards transport. The interaction between morphology, wave-driven resuspension and tidal advection appears to merit further systematic study.

The erosion rate may also vary in space and time because of variations in the erodability of the bottom sediment. This may readily occur even if the underlying geology is uniform: in regions where large amounts of sediment is deposited in each tidal cycle, it may not have a chance to consolidate fully before being re-eroded, and so will constitute a readily erodible 'patch' of bottom sediment. Again, the interaction of such erodible patches with advection may be rather complex; it is interesting to note, though, that the study by Friedrichs et al. (1998) suggested that such an erodible patch could account for the persistent turbidity maximum in some estuaries, and that it was in fact necessary for these systems to be morphodynamically stable.

In a mature morphodynamic system, not only may other processes act to balance the onshore movement of transport by settling lag, but the bathymetry of the system itself may adjust so that it tends to reduce such transport. The details of this adjustment remain an open question, but a number of mechanisms have been proposed, and it seems likely that in any real system several will combine to determine the morphology and resulting transport. Some of these can be put into the context of settling lag. For example, Friedrichs (1995) surveyed a range of tidal systems, and found that peak velocities tended to be nearly uniform along the channel: this would reduce the tendency of settling lag to import sediment to regions of low erosion, though it is known that in other contexts it does not necessarily eliminate it (see e.g. Pritchard and Hogg, Sect. 3.2.3 and 3.2.4). Changes in the width of the channel as the water level changes may also be significant: the presence of substantial intertidal flats may substantially alter the flood- or ebb-dominance of a tidal system (Dronkers 1986; Friedrichs and Aubey 1988), providing one example of a complex feedback between basin hypsometry, tidal distortion and sediment transport (c.f., for example, Boone and Byrne 1981). Unravelling such feedbacks appears to be an area in which a continuing interaction between simple models, numerical simulations and field observations is essential.

5 Summary and conclusions

We have constructed solutions for the tidal variation of suspended sediment concentrations and the resulting residual transport in a class of model tidal embayments. These results are highly idealised; however, the benefit of this idealisation is that we are able to identify clearly the role of various mechanisms which contribute to residual transport. This study, therefore, should be seen as an elucidation of the classic conceptual models developed by van Straaten and Kuenen (1958) and Postma (1961) and others, rather than as a tool for detailed predictive modelling.

The strongest conclusion to be drawn from our results is that including advective transport is crucial to investigating the variation of SSC in these embayments, and consequently that models (or model interpretations) which take account only of local processes are unlikely to predict residual transport reliably. This is the case even for relatively coarse sediment which is strongly controlled by local processes, because residual transport is sensitive to the small biases introduced through advection. While our model is not identical in some details to that originally employed by van Straaten and Kuenen (1958), it does suggest that the mechanism of settling lag which they originally proposed is a reasonable interpretation of the processes in short embayments. (Some subtleties involved in van Straaten and Kuenen's 'particle-following' model have been discussed by Pritchard and Hogg (2003), and we will not repeat this discussion here.)

Our model further illustrates the competition which can occur between externally imposed and internally generated overtides to determine the direction of residual transport, and it confirms that for fine sediment, settling lag generally tips the balance in favour of landwards transport. As in other tidal situations, what constitutes 'fine' sediment is determined by the quantity $\gamma \hat{w}_s \hat{T}/\hat{d}$,which measures the ratio of the tidal period to the sediment response timescale. Our model further illustrates the weak but detectable role of scour lag in enhancing landwards residual transport when advective contributions to transport are relatively weak.

One point which is brought out by this model and which has not been much commented on previously is the role of the parameter β which represents the vertical distribution of sediment in the water column and effectively controls the relative importance of advective transport. Depending on how strongly stratified the flow field and suspension are, different mechanisms may gain or lose influence over residual transport: in particular, when $\beta \neq 1$ systematic residual fluxes of sediment arise due to the differential advection of sediment and water. These findings indicate the importance of continuing detailed theoretical and field studies of sediment distribution in the water column.

In summary, the dynamics of short tidal embayments, as well as being of interest in themselves, provide a useful 'laboratory' in which the fundamental processes of residual sediment transport under tides can be investigated and understood. The results of the present study have illustrated that, 50 years after they were first identified, the physical processes leading to residual transport remain fascinating and subtle; we believe that the results presented here may augment those of more empirical investigations to develop our understanding of them further.

Acknowledgements This work was supported by the NERC/EPSRC Environmental Mathematics and Statistics Programme through a postdoctoral fellowship, ref. NE/B50188X/1. I am grateful for the very useful comments from Carl Friedrichs and from an anonymous referee, which helped to improve this paper substantially.

References

Bass SJ, Aldridge JN, McCave IN, Vincent CE (2002) Phase relationships between fine sediment suspensions and tidal currents in coastal seas. J Geoph Res 107(C10):3146 DOI 10.1029/2001JC001269

Boon JD, Byrne RJ (1981) On basin hypsometry and the morphodynamic response of coastal inlet systems. Mar Geol 40:27–48

Bolla Pitaluga M, Seminara G (2003) Depth-integrated modelling of suspended sediment transport. Wat Res 39(5):1137 DOI 10.1029/2002WR001306

Cancino L, Neves R (1999) Hydrodynamic and sediment suspension modelling in estuarine systems. Part II: application to the Western Scheldt and Gironde estuaries. J Mar Syst 22:117–131

Dronkers J (1986) Tidal asymmetry and estuarine morphology. Neth J Sea Res 20(2–3):117–131

Friedrichs CT, Aubrey DG (1988) Non-linear tidal distortion in shallow well-mixed estuaries: a synthesis. Est Coast Shelf Sci 27:521–545

Friedrichs CT (1995) Stability shear stress and equilibrium cross-sectional geometry of sheltered tidal channels. J Coast Res 11(4):1062–1074

Friedrichs CT, Armbrust BD, de Swart HE (1998) Hydrodynamics and equilibrium sediment dynamics of shallow, funnel-shaped tidal estuaries. In: Dronkers J, Scheffers M (eds) Physics of Estuaries and Coastal Seas. Balkema, Amsterdam, pp 315–327

Groen P (1967) On the residual transport of suspended matter by an alternating tidal current. Neth J Sea Res 3:564–574

Hoitink AJF, Hoekstra P, van Maren DS (2003) Flow asymmetry associated with astronomical tides: implications for the residual transport of sediment. J Geoph Res 108(C10):3315 DOI 10.1029/2002JC001539

Jung KT, Jin JY, Kang H-W, Lee HJ (2004) An analytical solution for the local suspended sediment concentration profile in tidal sea region. Est Coast Shelf Sci 61:657–667

Nichols MM, Biggs RB (1985) Estuaries. In: Davis R (ed) Coastal sedimentary environments, Chap 2. Springer, Berlin Heidelberg New York

Partheniades E (1965) Erosion and deposition of cohesive soils. J Hydr Div ASCE 91(HY1):105–139

Pethick JS (1980) Velocity surges and asymmetry in tidal channels. Est Coast Mar Sci 11:331–345

Postma H (1961) Transport and accumulation of suspended matter in the Dutch Wadden Sea. Neth J Sea Res 1:148–190

Prandle D (1997) Tidal characteristics of suspended sediment concentrations. J Hydr Eng 123(4):341–350

Pritchard D, Hogg AJ (2003) Cross-shore sediment transport and the equilibrium morphology of mudflats under tidal currents. J Geoph Res 108(C10):3313 DOI 10.1029/2002JC001570

Ridderinkhof H (1998) On the sensitivity of the large scale transport and distribution of fine-grained sediments in a tidal basin to the formulation of the erosion–sedimentation cycle. In: Dronkers J, Scheffers M (eds) Physics of Estuaries and Coastal Seas. Balkema, Amsterdam, pp 145–153

Ross MA, Mehta AJ (1989) On the mechanics of lutoclines and fluid mud. J Coast Res SI 5:51–61

Schuttelaars HM, de Swart HE (1996) An idealised long-term morphodynamic model of a tidal embayment. Eur J Mech B Fluids 15(1):55–80

Shi Z (2004) Behaviour of fine suspended sediment at the North passage of the Changjiang Estuary, China. J Hydrol 293:180–190

Shi Z, Ren LF, Zhang SY, Chen JY (1997) Acoustic imaging of cohesive sediment resuspension and re-entrainment in the Changjiang Estuary, East China Sea. Geo Mar Lett 17:162–168

Smith R (1977) Long-term dispersion of contaminants in small estuaries. J Fluid Mech 82:129–146

van de Kreeke J, Hibma A (2005) Observations on silt and sand transport in the throat section of the Frisian Inlet. Coastal Eng 52:159–175

van Straaten LMJU, Kuenen PH (1958) Tidal action as a cause of clay accumulation. J Sediment Petrol 28:406–413

Weeks AR, Simpson JH, Bowers D (1993) The relationship between concentrations of suspended particulate matter and tidal processes in the Irish Sea. Con Shelf Res 13(12):1325–1334

Winterwerp JC (2001) Stratification effects by cohesive and non-cohesive sediment. J Geophys Res 106(C10):22559–22574

Young WR, Jones S (1991) Shear dispersion. Phys Fluids A 3(5):1087–1101